Nucleic Acids Research, 1996, Vol. 24, No. 22 **4487–4494**

DNA binding of *Jun* and *Fos* bZip domains: homodimers and heterodimers induce a DNA conformational change in solution

Matthias John[+], Raymond Leppik[1,§], Steven J. Busch[1,‡], Michèle Granger-Schnarr and Manfred Schnarr*

Institut de Biologie Moléculaire et Cellulaire du CNRS, UPR 9002, 15, rue René Descartes, 67084 Strasbourg Cedex, France and [1]Marion Merrell Dow Research Institute, 16, rue d'Ankara, 67080 Strasbourg Cedex, France

Received August 2, 1996; Revised and Accepted September 26, 1996

ABSTRACT

We constructed plasmids encoding the sequences for the bZip modules of c-*Jun* and c-*Fos* which could then be expressed as soluble proteins in *Escherichia coli.* The purified bZip modules were tested for their binding capacities of synthetic oligonucleotides containing either TRE or CRE recognition sites in electrophoretic mobility shift assays and circular dichroism (CD). Electrophoretic mobility shift assays showed that bZip *Jun* homodimers and bZip *Jun*/*Fos* heterodimers bind a collagenase-like TRE (CTGACTCAT) with dissociation constants of respectively 1.4×10^{-7} M and 5×10^{-8} M. As reported earlier [Patel *et al.* (1990) *Nature* 347, 572–575], DNA binding induces a marked change of the protein structure. However, we found that the DNA also undergoes a conformational change. This is most clearly seen with small oligonucleotides of 13 or 14 bp harboring respectively a TRE (TGACTCA) or a CRE (TGACGTCA) sequence. In this case, the positive DNA CD signal at 280 nm increases almost two-fold with a concomitant blue-shift of 3–4 nm. Within experimental error the same spectral changes are observed for TRE and CRE containing DNA fragments. The spectral changes observed with a non-specific DNA fragment are weaker and the signal of free DNA is recovered upon addition of much smaller salt concentrations than required for a specific DNA fragment. Surprisingly the spectral changes induced by *Jun*/*Jun* homodimers are not identical to those induced by *Jun*/*Fos* heterodimers. However, in both cases the increase of the positive CD band and the concomitant blue shift would be compatible with a B to A-transition of part of the binding site or a DNA conformation intermediate between the canonical A and B structures.

INTRODUCTION

The AP-1 protein complex is a eukaryotic transcription factor that binds DNA in a sequence specific manner. AP-1 was first identified by its role in the regulation of the human metallothionein II_A gene, and soon after it was shown that c-*Jun* and c-*Fos* are constituents of AP-1. Several related genes of *Jun* and *Fos* exist, giving rise to the families of either the *Jun* transcription factors or the *Fos* transcription factors. These members of the AP-1 family associate with each other to form a variety of homo- or heterodimeric complexes. A hallmark of AP-1 became its ability to mediate gene induction by the phorbol ester tumor promoter 12-*O*-tetradecanoylphorbol-13-acetate (TPA) and led to the name TRE (TPA response element) for its 7 bp recognition site (TGA(C/G)TCA), which is present in numerous promoters. The same sequence is recognized by the transcriptional activator GCN4, which is involved in the regulation of amino acid biosynthesis in yeast. Binding of AP-1 to the TRE sequence can modulate transcription both positively and negatively (for a review see 1). The 8 bp recognition site CRE (cAMP responsive element) (TGACGTCA) is also a target for *Jun*/*Jun* or *Jun*/*Fos* complexes (2,3).

Jun and *Fos* belong to the bZip group of transcription factors, containing a DNA binding domain with clustered basic amino acids (b) and an adjacent leucine zipper motif (Zip) responsible for the dimerization of the transcription factors (for a review on bZip proteins see 4). The leucine zipper mediated dimerization of AP-1 proteins is concentration dependent and leads to increased α-helical secondary structure (5,6). Even as dimers, the basic domain of each monomer remains essentially unstructured in solution. In the presence of DNA, the basic region adopts an α-helical conformation as a consequence of recognition and binding to the consensus sequence (5). The crystal structure of the c-*Jun*/c-*Fos* bZip domain bound to a TRE sequence (7) showed that both subunits form continuous parallel α-helices. The C-terminal leucine zipper forms a coiled-coil structure. Both

* To whom correspondence should be addressed. Tel: +33 388 41 70 64; Fax: +33 388 60 22 18; Email: schnarr@ibmc.u-strasbg.fr

Present addresses: [+]Harvard Medical School, Department of Biological Chemistry and Molecular Pharmacology, 240 Longwood Ave., Boston, MA 02115, USA, [§]Department of Physical Biochemistry, National Institute for Medical Research, The Ridgeway, Mill Hill, London NW7 1AA, UK and [‡]Marion Merrel Dow Research Institute, 2110 E. Galbraith Road, Cincinnati, OH, USA

subunits make base-specific contacts with DNA in the major groove via their basic N-terminal regions. These contacts are essentially the same as those observed for the GCN4 bZip domain bound to a TRE (8) or a CRE sequence (9,10). In the latter case at least, the DNA undergoes a marked conformational change including features reminiscent of A-DNA (C3′-endo conformation for certain deoxyriboses and an average base-pair displacement of –1.4 Å). In the crystal structures of the GCN4-TRE and the *Jun*/*Fos*-TRE complexes, the DNA stays apparently closer to the B-conformation (7,8), although the average base pair displacement for the GCN4-TRE complex is far from neglectable (–0.9 Å) (11). In addition the unit vector normal to the base pairs also deviates substantially from canonical B-DNA (9). Weiss *et al.* (12) have shown that the circular dichroism spectrum of both a TRE or a CRE containing DNA is markedly increased upon addition of the GCN4 bZip domain. A similar change has not been reported for the bZip domains of *Jun* and *Fos* (5). Here we show that the bZip domains of *Jun* and *Fos* also induce a marked increase in the CD spectra of a series of double-stranded oligonucleotides containing TRE and CRE sites. Within experimental error the spectra of a bound TRE and a bound CRE are identical. On the contrary, a *Jun*/*Jun* complex induces a somewhat more pronounced spectral change than a *Jun*/*Fos* complex for both TRE and CRE binding sites. These results were obtained with recombinant bZip domains of c-*Jun* and c-*Fos* which are expressed as soluble proteins in *Escherichia coli*, and which do not contain any of the foreign helper sequences generally used for affinity purification.

MATERIALS AND METHODS

Plasmids

The mouse c-*Jun* gene was first digested with *Sma*I and *Pst*I. The resulting 0.94 kb DNA fragment was purified and redigested with *Hin*fI and *Ban*I. The *Hin*fI/*Ban*I fragment codes for the bZip domain of mouse c-*Jun* spanning amino acids 250 to 327, a sequence that is identical to human c-*Jun* 247 to 324. This *Hin*fI/*Ban*I fragment was cloned into the *Eco*RI/*Hin*dIII site of plasmid pKK223–3 (Amp^R; Pharmacia, Uppsala, Sweden) giving rise to plasmid pKK-*Jun*. The synthetic oligonucleotide linkers (Table 1) I (front end) and II (back end) were used to insert the *Jun* fragment into the vector. A 1.2 kb *Pvu*II fragment of the human c-*Fos* gene was recut with *Hin*fI and *Sau*3A. This fragment codes for the human c-*Fos* bZip domain, spanning amino acids 137 to 208. The *Hin*fI/*Sau*3A DNA was cloned into the same *Eco*RI/*Hin*dIII sites using linkers III (front end) and IV (back end), to give plasmid pKK-*Fos*.

Protein expression and purification

Plasmids pKK-*Fos* and pKK-*Jun* were transformed into *E.coli* strain RB791 (13). The bacteria harboring the pKK-*Fos* plasmid were grown in LB medium (10 g/l Bacto-tryptone, 5 g/l yeast extract, 10 g/l NaCl, 100 mg/l ampicillin) at 37°C. Bacteria transformed with the corresponding pKK-*Jun* plasmid expressed higher amounts of $Jun_{247–324}$ protein in minimal medium as compared with LB medium. These transformants were grown at 37°C in M9 medium (8.5 g/l $Na_2HPO_4{\cdot}2H_2O$, 3 g/l KH_2PO_4, 0.5 g/l NaCl, 1 g/l NH_4Cl pH 7.4, 50 mg/l ampicillin) supplemented with 0.4% (w/v) glucose, 1 mM $MgSO_4$, 50 µM $CaCl_2$, and 2 µM thiamin. In both cases, an overnight starter culture was diluted 10-fold and incubated until A_{550} = 0.8. Gene expression was induced with 1 mM ITPG, the cells grown for another 3 h, and harvested by centrifugation. About 12 g of wet bacterial paste was resuspended in 48 ml CED-0.3 buffer (300 mM NaCl, 20 mM citric acid, 10 mM EDTA, 5 mM DTT, pH 5). The lysis buffer was supplemented with 1 mM PMSF, 1 mM benzamidine, 1 µM pepstatin, 5 µM aprotinin; all further purification steps using CED buffer were done in presence of 1 mM PMSF only. Cells were disrupted with a French press at 500 kg/cm^2 pressure. The cleared supernatant was batch-incubated overnight with 15 ml of CED-0.3 equilibrated Heparin Ultrogel (IBF, Villeneuve-la-Garonne, France) at 4°C. The suspension was transferred to a column and washed with CED-0.3. A linear gradient using CED-0.3 and CED-2 (2 M NaCl, 20 mM citric acid, 10 mM EDTA, 5 mM DTT, pH 5; 1 mM PMSF) was applied to elute the proteins at a flow rate of 1 ml/min. The collected fractions were analyzed using SDS–PAGE. Ammonium sulfate was gradually added to the pooled bZip fractions under stirring up to 80% saturation. The precipitated proteins were dissolved in HPLC buffer A (0.05% TFA/H_2O) and injected on a semipreparative C-4 reversed phase coloumn (Macherey Nagel, Düren, Germany). A linear gradient between 32% and 40% HPLC buffer B (0.05% TFA in acetonitrile) was applied at a flow rate of 2 ml/min. The collected proteins were lyophilized and redissolved in deionized water. Protein concentration was determined according to Scopes (14) and the proteins were stored at –20°C in the presence of 5 mM DTT to avoid cysteine oxidation.

Table 1. Linkers used for cloning into plasmids

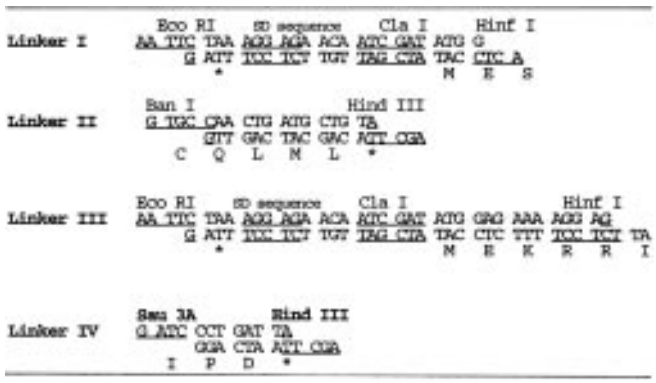

Oligonucleotides

Oligonucleotides were synthesized on an Applied Biosystems synthesizer and the resulting single-stranded DNA purified by C-18 reversed phase HPLC. Equimolar amounts of complementary strands were annealed in TE (10 mM Tris, 1 mM EDTA, pH 7.9). Samples were injected on an analytical size exclusion HPLC column (SEC-2000, Beckman, Fullerton, CA, USA) equilibrated with phosphate buffered saline (PBS; 150 mM NaCl, 10 mM Na-phosphate, pH 7.0). Those samples containing more than 5% of single stranded DNA contaminants were purified on a SEC-2000 column, the collected fractions of dsDNA were ethanol precipitated, dried and redissolved in TE buffer.

Electrophoretic mobility shift assay

Proteins at varying concentrations were incubated with about 2500 c.p.m. of ^{32}P-labeled oligonucleotides in 10 µl total sample

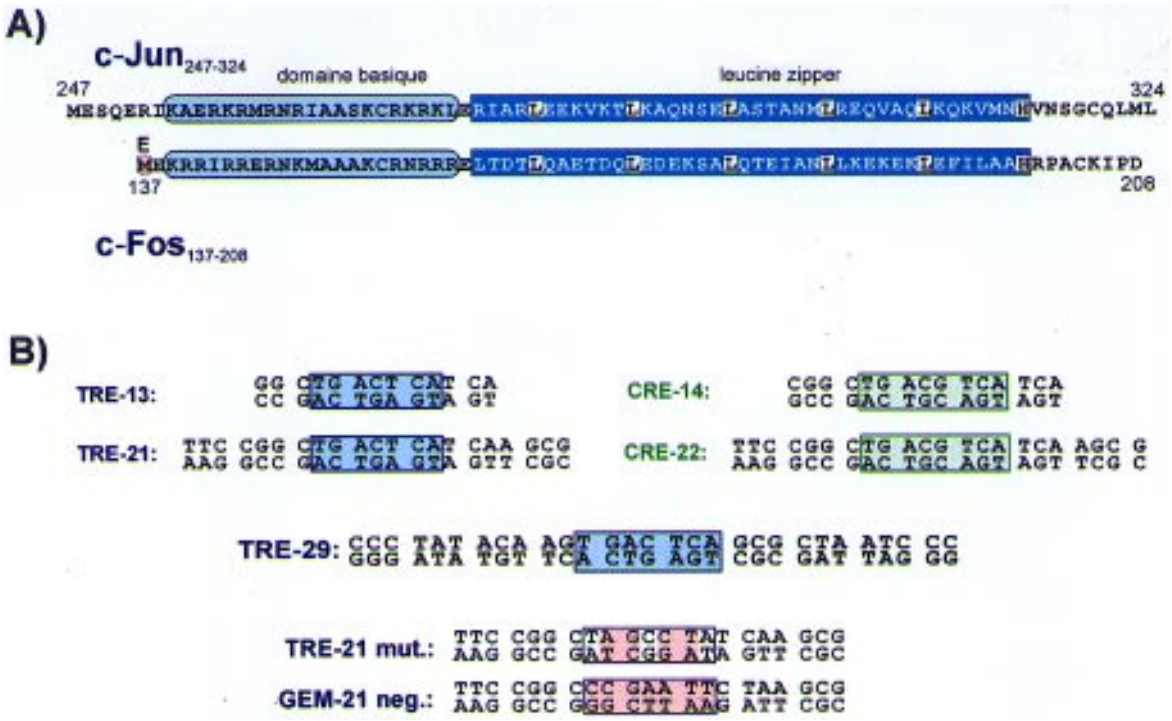

Figure 1. Sequence of the recombinant c-*Jun*$_{247–324}$ and c-*Fos*$_{137–208}$ bZip proteins. The first amino acid of c-*Fos*$_{137–208}$ was changed from Glu to Met (**A**). The oligonucleotides used in this study differ in length and contained either the TRE or CRE consensus sequence (boxed). Two oligonucleotides were synthesized as control. TRE-21 mut. contains one purine pair inversion and one pyrimidine pair inversion in the consensus site and retained some residual protein binding activity. In contrast to TRE-21 mut., no specific binding affinity of the bZip proteins for oligonucleotide GEM-21 neg. could be detected in EMSA. The control sequence of GEM-21 neg. is completely randomized as compared with TRE-21 (**B**).

volume. Equimolar amounts of separately purified *Jun* and *Fos* peptides were associated by an incubation of 30 min at 25°C prior to the formation of the protein–DNA complex. Under these conditions heterodimer formation and subunit exchange of *Jun* and *Fos* bZip domains occurs with a half-life of less than 10 s (15). The DNA interaction buffer contained 50 mM Tris–HCl, pH 8.0, 5 mM $MgCl_2$, 5 mM DTT, 1 mM EDTA, 10% glycerol, 0.1% Nonidet P-40, 2 µg of bovine serum albumin, and 0.1 µg of poly(dI-dC). The reaction mixtures were incubated for 30 min at room temperature and subsequently run on a 5% polyacrylamide gel (with 1:19 bisacrylamide) at 4°C. The running buffer was 0.5× TBE (45 mM Tris, 45 mM Borate, 1 mM EDTA, pH 8.3). The data were analyzed using either a Fuji 600 phosphoimager or a BioRad video scanning system.

Circular dichroism studies

CD spectra were recorded on a Jobin Yvon dichrograph under constant nitrogen flush at room temperature. The spectra were recorded between 200 and 320 nm using 1 mm or 10 mm path-length quartz cells (Hellma, Müllheim, Germany). The proteins were dissolved in PBS-200 (200 mM NaCl, 10 mM Na-phosphate pH 7.5, 1 mM DTT) buffer. The spectra presented here represent the baseline corrected mean of at least three scans of the same sample. A starting concentration of 0.04 mg/ml of oligonucleotide was used for the protein titration experiments. Equal volumes of protein stock solutions were added until a maximum of DNA signal change was obtained. The relative signal changes were corrected for dilution, which was kept beneath 3%. The DNA CD spectra (Fig. 5**)** show the absolute signal change without correction for dilution.

RESULTS

Expression and purification of soluble *Jun* and *Fos* bZip domains

The sequences of the overexpressed bZip modules c-*Jun*$_{247–324}$ and c-*Fos*$_{137–208}$ are shown in Figure 1. Using the pKK plasmids, we were able to obtain entirely soluble recombinant proteins which could be isolated without the need to use denaturing conditions. These two proteins differ only slightly in sequence length from those used in previous studies (5), but they lack the six histidine tag. It is possible that this His_6-tag is responsible for the aggregation and precipitation of the recombinant *Jun* and *Fos* proteins in *E.coli* studied earlier (5,16). After cell lysis, the proteins were purified in a first step by ion exchange chromatography using a heparin ultrogel column. The chosen buffer system suppressed the strong proteolytic degradation which was observed at neutral to alkaline pH values. As the final purification step, we used a C-4 reversed phase HPLC column. The purity of c-*Jun*$_{247–324}$ and c-*Fos*$_{137–208}$ was monitored on 12% SDS-polyacrylamide gels, and by HPLC on a C-18 analytical reversed phase column. Both methods indicated for c-*Jun*$_{247–324}$ and c-*Fos*$_{137–208}$ a protein purity greater than 95% (Fig. 2). Mass spectral analysis showed that both proteins had the correct molecular weights (c-*Jun*$_{247–324}$, found: 9136.1, calculated: 9138.8; c-*Fos*$_{137–208}$, found 8520, calculated: 8521).

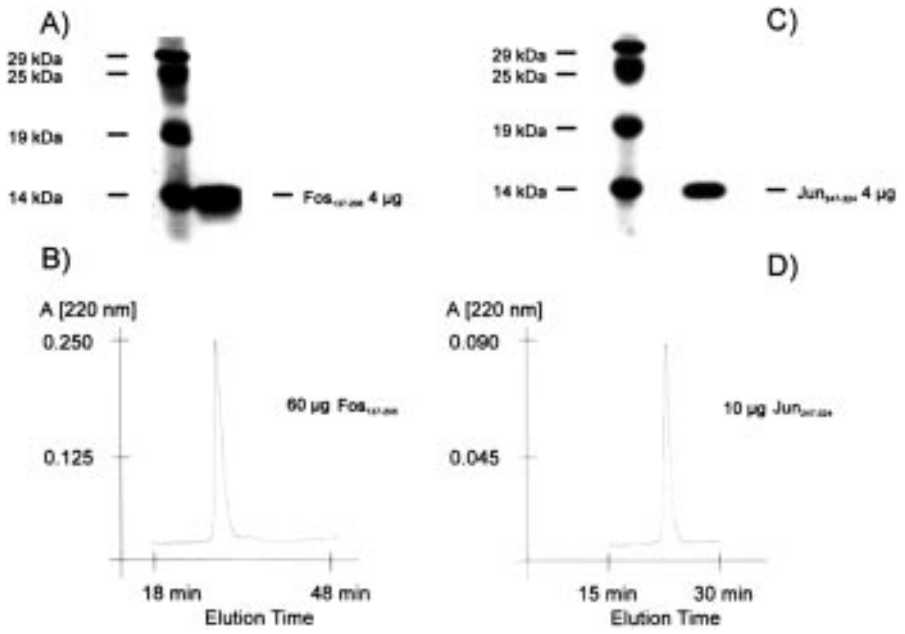

Figure 2. Purity of c-*Jun*$_{247–324}$ and c-*Fos*$_{137–208}$ proteins after ion exchange chromatography and reversed phase HPLC purification. (**A**) and (**C**) show the Coomassie-stained 12% acrylamide gels charged with 4 µg of purified protein. (**B**) and (**D**) show the elution profile of c-*Fos*$_{137–208}$ and c-*Jun*$_{247–324}$, respectively, on a C18 analytical HPLC column. The complementary runs with 10 µg c-*Fos*$_{137–208}$ and 60 µg c-*Jun*$_{247–324}$ are not shown here, but did not reveal detectable contaminants either.

DNA binding of c-*Jun*$_{247–324}$ and c-*Fos*$_{137–208}$

The DNA binding capacity of the bZip modules were tested in electrophoretic mobility shift assays (EMSA). For this purpose we used synthetic oligonucleotides of different length (Fig. 1B). One series of oligonucleotides contained a binding site derived from the collagenase TRE, whereas the other series harbored the corresponding CRE site. As a control, we used two oligonucleotides. TRE-21 mut. contained a mutated TRE site for which two base pairs in each TRE half-site were simply swapped. These changes in the recognition site were not sufficient to abolish protein binding activity completely, since some retarded DNA could be detected in EMSA. The other control oligonucleotide, GEM-21 contained a scrambled, non-palindromic sequence with the same number of G/C and A/T base pairs as the TRE consensus site. For this oligonucleotide no bound DNA was detectable in EMSA. All specific oligonucleotides formed well-defined complexes with both the *Jun*/*Jun* and *Jun*/*Fos* bZip domains.

The TRE-21 collagenase-like oligonucleotide was used to determine the equilibrium dissociation constant K_d of either the c-*Jun*$_{247–324}$ homodimer or the c-*Jun*$_{247–324}$/c-*Fos*$_{137–208}$ heterodimer DNA complex (Fig. 3). The K_d value corresponds approximately to the protein concentration necessary to bind 50% of the DNA if the protein is in large excess over the DNA concentration. For the c-*Jun*$_{247–324}$/c-*Fos*$_{137–208}$ complex 50% of bound DNA is reached upon addition of about 5×10^{-8} M of total protein concentration.

The c-*Jun*$_{247–324}$ homodimer reaches 50% DNA-binding for an ~3-fold higher protein concentration (1.4×10^{-7}M), suggesting an ~3-fold smaller DNA binding affinity as compared with the c-*Jun*$_{247–324}$/c-*Fos*$_{137–208}$ heterodimer. Additionally, the slope of the c-*Jun*$_{247–324}$ homodimer DNA binding isotherm (not shown) is flatter than that of the heterodimer for DNA saturation greater than 50%. Higher c-*Jun*$_{247–324}$ concentrations are thus required to reach full DNA binding. We are not aware of any other published determination of K_d values for DNA binding of *Jun* homodimers and/or *Jun*/*Fos* heterodimers. However, Abate *et al.* (17) determined an 8-fold smaller relative DNA binding affinity of a c-*Jun* bZip homodimer as compared with a c-*Jun*/c-*Fos* bZip heterodimer using a human metallothionein IIA-like TRE as DNA target. The reason we find a somewhat smaller difference (about 3-fold) using a collagenase-like TRE may be the difference in the bases flanking the TRE core sequence. Ryseck and Bravo (3) have shown indeed that the bases flanking the central TGACTCA sequence may strongly influence the DNA binding affinity especially of c-*Jun* homodimers. In particular a collagenase-like TRE (oligo 10 in their study) showed a high affinity for c-*Jun* homodimers, such that c-*Jun* homodimers and c-*Jun*/c-*Fos* heterodimers obtained a comparable DNA binding score (10–50% DNA binding) in their study (3).

Circular dichroism experiments

The bZip modules were further tested by circular dichroism spectroscopy. Circular dichroism is a useful structural tool for the characterization of both protein and nucleic acid conformation (for a recent review see ref. 18). Conformational changes induced upon formation of a protein–DNA complex may be generally attributed to one or the other species, since the composite spectrum is dominated by the DNA between 260–290 nm, and by the protein between 210–230 nm. In the following, protein CD spectra will be expressed as usual by the molar ellipticity Θ, whereas the DNA CD spectra are expressed as $\Delta\varepsilon = \varepsilon_L - \varepsilon_R$, where ε_L and ε_R represent the molar extinction coefficients of, respectively, left and right circularly polarized light. The numerical conversion between the two measures of CD is straightforward ($[\Theta] = 3298\ \Delta\varepsilon$).

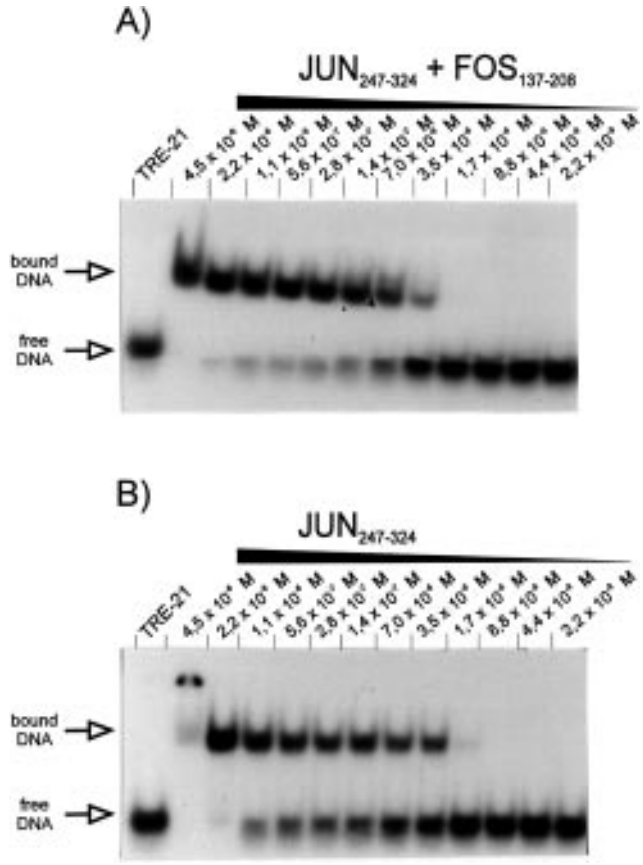

Figure 3. Electrophoretic mobility shift assay of TRE-21 with the c-*Jun*$_{247–324}$ / c-*Fos*$_{137–208}$ heterodimer (**A**) and the c-*Jun*$_{247–324}$/c-*Jun*$_{247–324}$ homodimer (**B**). The binding reactions were analyzed by native gel electrophoresis (5%) and subsequent autoradiography. The indicated concentrations correspond respectively to the concentration of (c-*Jun*$_{247–324}$ +c-*Fos*$_{137–208}$) monomers and c-*Jun*$_{247–324}$ monomers. The TRE-21 concentration at half-saturation was at least 30-fold smaller than the protein concentration.

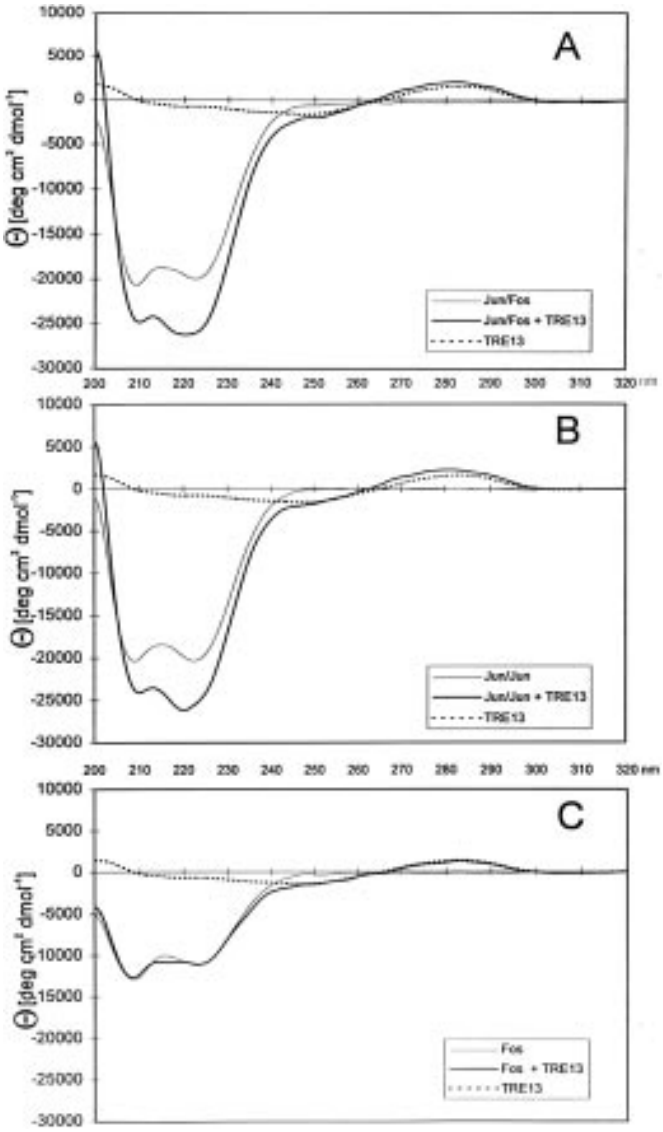

Figure 4. CD spectra of the three different protein and protein–DNA complexes. The protein concentration was 20 µM, the double stranded DNA concentration was 12 µM in PBS200 pH 7.5, containing 1 mM DTT.

At a concentration of 20 µM in PBS200, the c-*Jun*$_{247–324}$ homodimer and the c-*Jun*$_{247–324}$/c-*Fos*$_{137–208}$ heterodimer have Θ values at 222 nm of –20.000 degrees × cm^2 × dmol^{-1} (Fig. 4). Assuming a Θ value of –33.000 for 100% α-helical secondary structure (19,20), this indicates an α-helix content of about 60% for both the homo- and the heterodimer, corresponding quite closely to the fraction of amino acids being part of the leucine zipper (Fig. 1). The incomplete structure of the protein is thus most likely due to the disordered N-terminal basic region and possibly also a disordered C-terminal tail of the bZip modules. c-*Fos*$_{137–208}$ alone (Θ value of –11.000) appears to be only ~30% helical under these conditions. Furthermore, no DNA binding activity could be detected for c-*Fos*$_{137–208}$ neither in EMSA, nor in circular dichroism experiments (Fig. 4).

Figure 4 shows further that upon addition of DNA, the c-*Jun*$_{247–324}$ homodimer and the c-*Jun*$_{247–324}$/c-*Fos*$_{137–208}$ heterodimer show a significant increase in the magnitude of the helix-associated bands at 208 and 222 nm. The increase from Θ = –20.000 to about –26.000 corresponds to a gain in α-helicity of ~18% corresponding to ~14 additional amino acids folding into an α-helical structure upon formation of the protein–DNA complex. This value is compatible with a coil–helix transition of the part of the basic domain being in direct contact with the DNA (Fig. 1). Using His-tagged *Jun* and *Fos* subdomains, being respectively 33 and 24 amino acids longer than those used in this study, Patel *et al.* (5) have observed an increase of helicity of only 10%. Given the greater length of their bZip domains, this corresponds to a transition of 10–12 amino acids from an essentially denatured to an α-helical state upon DNA binding in reasonable agreement with the value reported here. c-*Fos*$_{137–208}$ alone does not exhibit an increase in α-helicity upon DNA binding (Fig. 4C)

Fos and *Jun* bZip domains induce a DNA conformational change

Formation of the protein–DNA complex not only induces a conformational change of the bZip modules, but also changes the

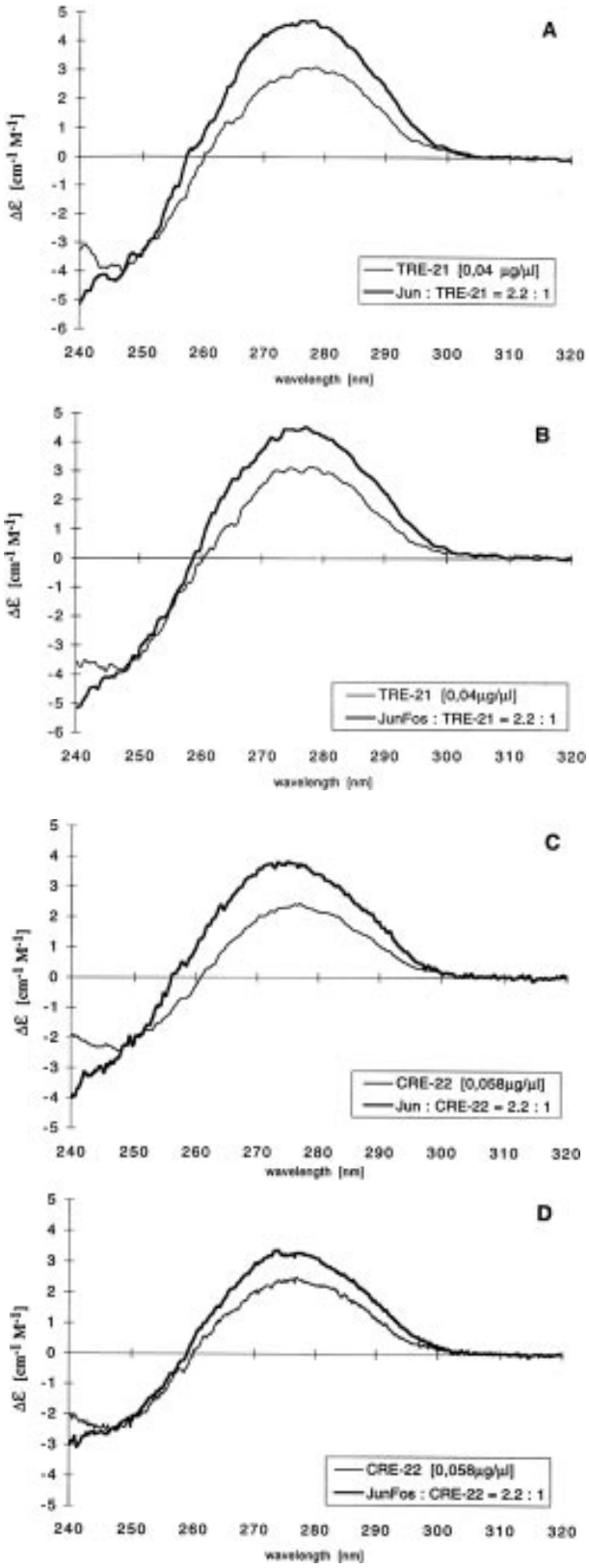

Figure 5. CD Spectra of TRE-21 and CRE-22 in the absence and presence of the *Jun* and *Fos* DNA binding domains. (**A**) and (**C**) c-$Jun_{247–324}$ homodimer, (**B**) and (**D**) c-$Jun_{247–324}$/c-$Fos_{137–208}$ heterodimer. The molar ratios of protein to duplex DNA are indicated in the boxes. The initial DNA concentration was 0.04 µg/µl (2.9 µM).

DNA CD spectra, indicating changes in the conformation of the DNA. Addition of either the c-$Jun_{247–324}$ homodimer or the c-$Jun_{247–324}$/c-$Fos_{137–208}$ heterodimer leads to a shift of the oligonucleotide spectra towards lower wavelength and a marked increase in signal intensity of the positive CD band at 280 nm.

Figure 5A and B show the CD spectra of TRE-21 in the absence and presence of the bZip domains. The c-$Jun_{247–324}$/c-$Fos_{137–208}$ heterodimer (B) leads to a slightly less pronounced signal increase than the c-$Jun_{247–324}$ homodimer (A), i.e. an increase of 1.48-fold at 280 nm instead of 1.65-fold, respectively.

Figure 5C and D show the corresponding spectra of CRE-22. Again, the heterodimer induces a somewhat smaller change in the DNA spectrum than the c-$Jun_{247–324}$ homodimer (1.45-fold instead of 1.58-fold). The spectral changes for both complexes are even more pronounced for CRE-14 (*Jun*/*Jun* 1.75-fold; *Jun*/*Fos* 1.6-fold) and TRE-13 (*Jun*/*Jun* 1.75-fold; *Jun*/*Fos* 1.6-fold). This may principally reflect the difference in length of the two pairs of double-stranded oligonucleotides.

Assuming that the spectral changes are mostly due to specific protein binding to the TRE and CRE elements within the oligonucleotides of length l = 13, 14, 21, 22 and 29 base pairs (Fig. 1), one would indeed expect that only a segment of n base pairs would be pertubed upon protein binding, whereas the remaining (l – n) base pairs would stay in a canonical, most likely B-conformation, i.e.:

$$\Delta\varepsilon_{max} = n/l \cdot \Delta\varepsilon_n + (l - n)/l \cdot \Delta\varepsilon_0 \quad \mathbf{1}$$

with $\Delta\varepsilon_{max}$ being the observed signal upon complex formation under saturating conditions, $\Delta\varepsilon_n$ the signal of the perturbed base pairs, and $\Delta\varepsilon_0$ the signal of the unperturbed base pairs. This equation predicts a linear relationship between $\Delta\varepsilon_{max}/\Delta\varepsilon_0$ and $1/l$, i.e:

$$\Delta\varepsilon_{max}/\varepsilon_0 = (n \cdot \Delta\varepsilon_n/\Delta\varepsilon_0 - n) \cdot (1/l) + 1 \quad \mathbf{2}$$

Figure 6A shows that a plot of $\Delta\varepsilon_{max}/\Delta\varepsilon_0$ versus $1/l$ does indeed exhibit a linear relationship for both the $Jun_{247–324}$ homodimer and the *Jun* $_{247–324}$/$Fos_{137–208}$ heterodimer complex, and that the homodimer induces consistently larger signal changes than the heterodimer.

Figure 6B shows the relative increase of the CD signal ($\Delta\varepsilon/\Delta\varepsilon_0$) at 280 nm as a function of the protein/DNA ratio. The addition of *Jun* and *Jun*/*Fos* bZip domains leads to an essentially linear change of the DNA CD signal, suggesting that binding is stoichiometric under these conditions. The titration curve of TRE-13 shows that the intensity increase reaches a maximum at a molar ratio of about two protein monomers per DNA duplex for both protein complexes, which is in good agreement with the expected stoichiometry. This indicates further that the proteins are fully active in DNA binding.

These CD signal changes are completely reversible. The addition of NaCl to the reaction mixture leads to a complete suppression of the effect (Fig. 7) suggesting that both complexes are sensitive to salt as expected from the numerous salt bridges formed between the basic region and the DNA phosphates (see ref. 5). The dissociation curve for the *Jun*/*Fos* complex is somewhat steeper than that of the *Jun*/*Jun* complex. Half-dissociation occurs at ~450 mM NaCl in the case of the heterodimer and at ~550 mM for the homodimer. Parallel to the signal decrease of the DNA at 280 nm, we also observed a signal decrease of the bZip proteins at 222 nm. This indicates a loss of α-helical conformation in the basic region of the proteins upon dissociation of the proteins from the TRE or CRE sequences. The non-specific control-duplex GEM-21

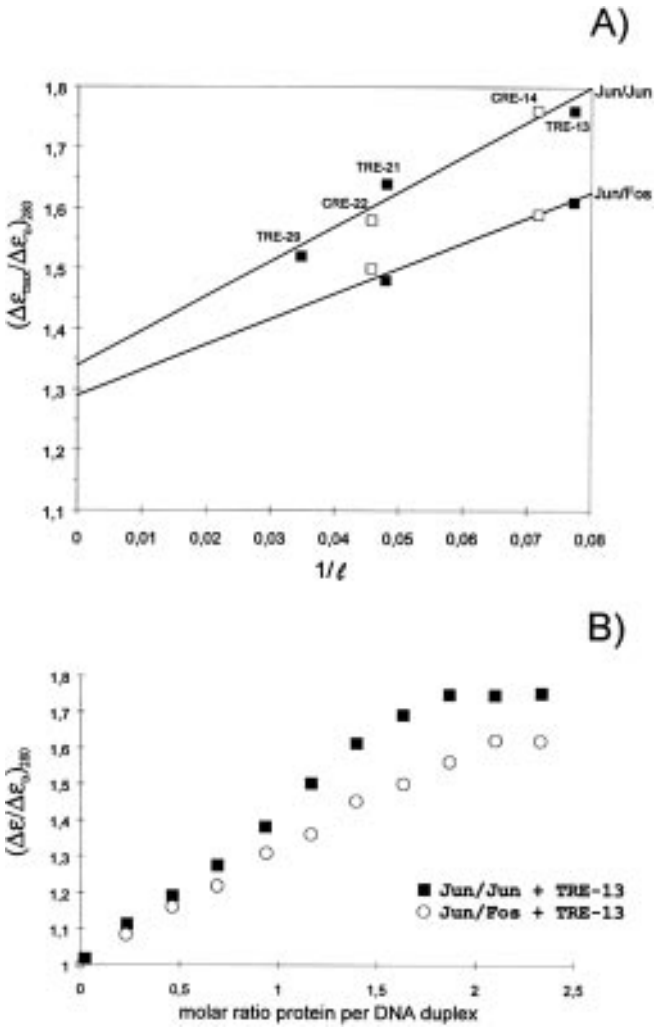

Figure 6. (**A**) Plot of the maximal CD signal change ($\Delta\varepsilon_{max}/\Delta\varepsilon_0$) versus the reciprocal oligonucleotide length (1/l). (**B**) CD signal change $\Delta\varepsilon/\Delta\varepsilon_0$ of TRE-13 as a function of protein concentration. DNA dilution effects upon addition of protein stock solutions are corrected. At a molar ratio of about two protein monomers per DNA duplex, the signal increase reaches its maximum. The DNA signal increase is more pronounced for the c-*Jun*$_{247–324}$ homodimer as compared with the c-*Jun*$_{247–324}$ /c-*Fos*$_{137–208}$ heterodimer.

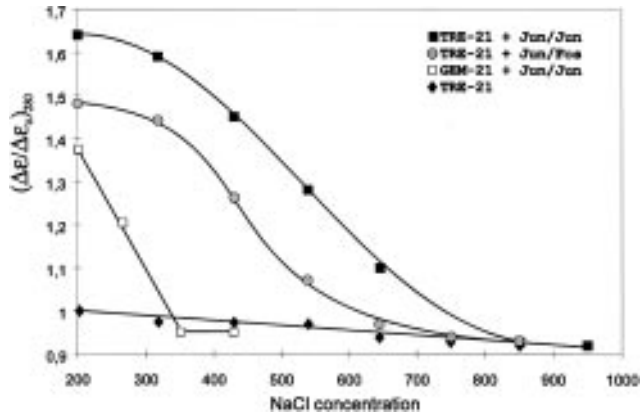

Figure 7. Salt dependence of the DNA CD signal increase. Upon addition of increasing amounts of NaCl the spectrum of free DNA is progressively restored.

shows a smaller increase in signal intensity (1.38-fold in the case of c-*Jun*$_{247–324}$ homodimer) and half-dissociation occurs at a much smaller salt concentration (275 mM). We observe a slight CD signal decrease of less than 10% for free TRE-21 at higher salt concentrations. For this reason, the NaCl titration leads to final signal intensities at 280 nm slightly below 1.

DISCUSSION

In this study we report the construction, overexpression and purification of the soluble bZip modules *Jun*$_{247–324}$ and c-*Fos*$_{137–208}$. Their secondary structure and their ability to bind oligonucleotides containing TRE or CRE sites were tested by using CD and EMSA, respectively. The CD measurements of protein dimers in the presence of stoichiometric amounts of double stranded oligonucleotides revealed different impacts of *Jun*/*Jun* and *Jun*/*Fos* bZip dimers on the DNA spectra. *Jun* homodimers changed the DNA signal of all four specific oligonucleotides to a somewhat stronger extent than *Jun*/*Fos* heterodimers suggesting that the homodimer might induce a more pronounced conformational change than the heterodimer. So far only the X-ray structure of a *Jun*/*Fos* bZip-TRE complex has been described (7).

The influence of c-*Jun* and c-*Fos* bZip domains on oligonucleotide conformation has not been reported in an earlier CD study (5). It is likely that a longer oligonucleotide was used in that study, which may have masked the DNA signal changes. In our study, the TRE-29 oligonucleotide spectrum is considerably less sensitive to protein binding than those of the shorter TRE-13 and CRE-14 oligonucleotides (Fig. 6A).

Kerppola and Curran (21–23) reported that *Jun* homodimers and *Jun*/*Fos* heterodimers bend DNA in opposite directions. The difference in the CD spectra induced by these two species is however unlikely to be linked to differential bending, since circular dichroism seems to be fairly insensitive to DNA bending (24). Using a DNA cyclization assay and EMSA experiments with different DNA constructs, Sitlani and Crothers (25) concluded recently that neither *Jun* homodimers nor *Jun*/*Fos* heterodimers induce substantial DNA bending.

The observed changes in the DNA CD spectra upon complex formation with the *Jun*, *Fos* and GCN4 bZip domains would however be compatible with the induction of a DNA structure related to the A-form. Upon addition of ethanol, DNA undergoes a B to A transition. Ivanov and Krylov (26) show a series of spectra with partial A-like character. The spectral changes observed for a transition from B-DNA to a situation where about 30% of the DNA adopts an A-structure would nicely match the changes which we observe upon complex formation with the *Jun* and *Fos* bZip domains, i.e. a ~2-fold increase of the CD intensity at 280 nm and a blue-shift of about 4nm.

For TRE-13 and CRE-14 this would correspond to ~4 bp in a pure A conformation, or more likely to an intermediate conformation between A and B over a longer stretch of the binding site. This kind of 'intermediate' structure has been described by Nekludova and Pabo (11) and applies also to the GCN4-CRE complex (9,10) which reveals structural features reminiscent of A-DNA as outlined above. Throughout the entire fragment, the average displacement of the base-pair centerline from the helical axis is

–1.4 Å (9) as compared with –4 to –5 Å for pure A DNA and no displacement for B-DNA (11). These features would be compatible with a partial B→A-like transition suggested by the CD spectral changes observed upon addition of the *Jun* and *Fos* bZip domains (this work) and GCN4 bZip domains (12).

Surprisingly, we observe the same structural changes in solution for both the CRE and the TRE complex, since the TRE structure in both the GCN4-TRE (8) and the *Jun*/*Fos*-TRE complex (7) has been described as being in the B-form. However, a reexamination of the GCN4-TRE structure by Nekludova and Pabo (11) revealed an overall displacement of –0.9 Å suggesting a significant deviation from canonical B-DNA. Nevertheless the CRE crystal structure within the GCN4 complex seems more A-like than the corresponding TRE structure (9). It might be that in solution the TRE structure within the complex is somewhat different than in the crystal and that TRE and CRE adopt essentially the same conformation in solution at least as far as base stacking is concerned.

ACKNOWLEDGEMENTS

We thank Paolo Sassone-Corsi for supplying the plasmids containing the c-*Jun* and c-*Fos* genes, Pierre Lepage for the mass spectral analyses and Annie Hoefft for synthesizing the oligonucleotides. M.J. was supported by a fellowship of the Gottlieb Daimler- and Karl Benz-foundation, Germany.

REFERENCES

1 Angel,P. and Karin,M. (1991) *Biochim. Biophys. Acta.* **1072**, 129–157.
2 Nakabeppu,Y. and Nathans,D. (1989) *EMBO J.* **8,** 3833–3841.
3 Ryseck,R.P., and Bravo,R. (1991) *Oncogene* **6,** 533–542.
4 Hurst,H. (1994) *Protein Profile* **1,** 123–166.
5 Patel, L., Abate,C., and Curran,T. (1990) *Nature* **347,** 572–575.
6 Schmidt-Dörr,T., Oertel-Buchheit,P., Pernelle,C., Bracco,L., Schnarr,M., and Granger-Schnarr,M. (1991) *Biochemistry* **30,** 9657–9664.
7 Glover,M.J.N., and Harrison,S.C. (1995) *Nature* **373,** 257–261.
8 Ellenberger,T.E., Brandl,C.J., Struhl,K., and Harrison,S.C. (1992) *Cell* **71,** 1223–1237.
9 Keller, W., König,P., and Richmond,T.J. (1995) *J. Mol. Biol.* **254,** 657–667.
10 König,P., and Richmond,T.J. (1993) *J. Mol. Biol.* **233,** 139–154.
11 Nekludova,L., and Pabo,C.O. (1994) *Proc. Natl. Acad. Sci. USA* **91,** 6948–6952.
12 Weiss,M.A., Ellenberger,T., Wobbe,C.R., Lee,J.P., Harrison,S.C., and Struhl,K. (1990) *Nature* **347,** 575–578.
13 Brent,R., and Ptashne,M. (1981) *Proc. Natl. Acad. Sci. USA* **78,** 4204–4208.
14 Scopes,R.K. (1974) *Anal. Biochem.* **59**, 277–282.
15 Patel,L.R., Curran,T., and Kerppola,T.K. (1994) *Proc. Natl. Acad. Sci. USA* **91,** 7360–7364.
16 Xanthoudakis,S. and Curran,T. (1994) *Methods Enzymol.* **234,** 163–175.
17 Abate,C., Luk,D., Gentz,R., Rauscher,F.J., and Curran,T. (1990) *Proc. Natl. Acad. Sci. USA* **87,** 1032–1036.
18 Woody,R.W. (1995) *Methods Enzymol.* **246,** 34–71.
19 Chen,Y.-H., Yang,J.T., and Chau,K.H. (1974) *Biochemistry* **13,** 3350–3359.
20 Zhong,L. and Johnson,W.C. (1992) *Proc. Natl. Acad. Sci. USA* **89,** 4462–4465.
21 Kerppola,T.K., and Curran,T. (1991) *Science* **254,** 1210–1214.
22 Kerppola,T.K., and Curran,T. (1991) *Cell* **66,** 317–326.
23 Kerppola,T.K., and Curran,T. (1993) *Mol. Cell. Biol* **13,** 5479–5489.
24 Sprous,D., Zacharias,W., Wood,Z.A. and Harvey,S. (1995) *Nucleic Acids Res.* **23,** 1816–1821.
25 Sitlani,A., and Crothers,D.M. (1996) *Proc. Natl. Acad. Sci. USA* **93,** 3248–3252.
26 Ivanov,V.I. and Krylov,Y. (1992) *Methods Enzymol.* **211,**111–127.